PREPARATION AND CHARACTERIZATION OF AMPHIPHILIC TITANIUM DIOXIDE NANOGEL COMPOSITES WITH HIGH PERFORMANCE IN WATER TREATMENT

A. M. ATTA[a,b*], H. A. AL-LOHEDAN[a], A. M. TAWFEEK[c], A. A. ABDEL-KHALEK[d]

[a]*Surfactants research chair, chemistry department, college of science, King Saud university, Riyadh, KSA.*

[b]*Petroleum Application department, Egyptian petroleum research institute, Cairo, Egypt*

[c]*College of science, king Saud university, Riyadh, KSA.*

[d]*Chemistry department, Faculty of Science, Beni Suef University, Beni Suef, Egypt.*

Titanium dioxide attracted great attention to apply as phodegradation catalyst to remove organic dyes without evaluation their removal efficiency as adsorbents. This work aims to increase the removal efficiency of TiO_2 by encapsulation into nanogel composites to facilitate its application for water treatment. The TiO_2nanogel composites were prepared by using dispersion crosslinking radical polymerization technique in mixed water ethanol solvent. The TiO_2 morphology and contents for its nanogel composites with polyacrylamides were determined as well as its ability to reduce water surface tension to adsorb at different interfaces. The prepared composites showed great ability to remove organic and inorganic pollutants from water with removal capacities ranged from 445 to 485 mg/g.

(Received November 18, 2015; Accepted January 13, 2016)

Keywords: water purification; Titanium dioxide; nanocomposites; dye; heavy metals.

1. Introduction

Toxic chemicals such as heavy metals and pathogens are hazardous for human health when contaminated with clean water. There are several methods applied to remove these pollutants from water such as physical treatments (adsorption, flocculation, ion exchange and membrane filtration), biological treatments and photo- catalysis [1-5]. The nanoscience and nanotechnology devolved new nanomaterials to overcome the disadvantages of common traditional methods used for water treatments such as transfer of pollutants from water to huge masses of adsorbents materials [7–9]. However, the availability and cost of production of nanomaterials limit their application in environmental remediation. The development of simple and economic routes to synthesize and apply nanomaterials for water treatment is one of the ultimate goals of nanoscience and nanotechnology for environmental applications. The most important characteristics of these nanomaterials are fast removal of pollutants and regeneration and reuse with the same removal efficiencies several times. One of the most useful techniques used to achieve this goal is incorporating of inorganic nanomaterials with organic polymers to increase the water permeability of active layer [10]. However, the diffusion rate of monomers to the interface increased to expand the wet zone on the top layer of nanocomposites [11]. Moreover, inorganic additives (e.g. titanium dioxide (TiO_2), silica, silver, and zeolite nanoparticles) have good antimicrobial activities and

*Corresponding author: aatta@ksu.edu.sa

fouling resistances that increase their applications as adsorbents for several types of water pollutants [12–17].

The nanomaterials have 3D nanostructures with discrete sizes, shapes and chemical functionalities especially that are most likely self-assembly have attracted much attention in different advanced technology and applications [18-20]. It is quite challenging to prepare 3D nanostructures having controlled sizes and dimensions from the building blocks (i.e., nanoparticles, nanorods, nanofibers, and nano-films). However, TiO_2 nanostructures based on nanotubes [21-23], nanowires [24], nanospheres [25, 26], and macro mesoporous materials [27, 28] have engaged great interest because of they have superior performances and varied morphologies. There are few reports synthesized TiO_2 spheres with hierarchical structures that were in catalysis and water treatments [29-32]. In previous works [33-36], the crosslinking technique to form nanogel composites succeeded to prepare sphere nano inorganic oxide nanogel composites have controlled morphologies and sized distribution. In this work, we report the simple controlled preparation of encapsulated nanogel composites contain TiO_2 spheres as a nanoparticle core and self-assembly nanogels using dispersion crosslinking polymerization technique. The poly (vinyl pyrrolidone), PVP, was used as dispersing agent in ethanol water solvent to disperse TiO_2 in the polymerization solution. Different types of acrylamide monomers were used to study the effect of monomer charges on the dispersability and assemble of nanoparticle into nanogel composites.

2. Experimental

2.1. Materials

Titanium dioxide (TiO_2; nano-powder was produced from Sigma-Aldrich Co. with average particle size 21 nm) was used as precursor to obtain nanogel composites. Acrylamide (AAm), sodium 2- acrylamido-2-methylpropane sulfonate (Na-AMPS; 50 wt. %), 3-acrylamidopropyl trimethylammonium chloride solution (APTAC; 75 wt. % in H_2O), poly (vinyl pyrrolidone), PVP; with molecular weight 40000 g/mol), N,N-methylenebisacrylamide (MBA), and radical initiator of ammonium persulfate (APS) were obtained from Aldrich Chemical Co and used without further purification. Deionized water (DI) and ethanol are analytical grades and used as solvent.

Stock solutions (1000 ppm) were prepared from MB, cobalt and nickel nitrates in aqueous solution.

Phosphate buffer solutions (PBS) having pH range 2 — 12 are used to study the performance of nanocomposites at different pH solutions.

2.2. Synthesis procedure

The TiO_2 nanogel composites based on AMPS-Na, AAm and their copolymers were synthesized by dispersion of TiO_2 (2 g) and PVP (0.3 g) in water/ethanol (60/40 vol %) for 24 h. AMPS-Na monomer (2 mL) or AAm (1g) was dissolved in the reaction mixture as well as APS (0.03 g), and MBA (0.03 g) under nitrogen gas atmosphere. The reaction temperature was increased up to 55 ^{o}C under stirring for 4 h. The dispersed TiO_2 PAMPS-Na or PAAm was isolated using ultra-centrifuge at 21000 rpm for 30 minute. The TiO_2nanogel composites washed five times with ethanol and dried under vacuum at 30 ^{o}C.

The same procedure was repeated to encapsulate TiO_2 into crosslinked copolymer nanogel composite based on PAMPS-Na/AAm and PAPTAC/AAm copolymers at equal mol ratios of reacted monomers.

2.3. Characterization

Transmittance electron microscope (TEM; JEOL JEM-2100 F has acceleration voltage of 200 kV) was used to detect the morphology of TiO_2 and their nanogel composites.

The surface morphology was evaluated and scanning electron microscope (SEM; JEOL 6510 LA SEM, JEOL, Japan).

The TiO_2 contents and thermal stability of TiO_2 nanogel composites were evaluated using thermogravimetric analyses (TGA-50 SHIMADZU) at a heating rate of 10 ◦C /min.

The dispersion stability of TiO_2nanogel composites and their surface charges were evaluated by measuring zeta potentials using Laser Zeta meter Malvern Instruments (Model Zetasizer 2000).

The surface activity of TiO_2 nanogels was determined from surface tension measurement in aqueous solution at 25 ^oC using drop shape analyzer model DSA-100.

The concentration of cobalt and nickel cations in aqueous solution was determined using atomic absorption spectroscopy (AAS; Perkin-Elmer 2380) in the direct aspiration into an air-acetylene flam.

2.4. Adsorption and desorption experiments

UV-visible spectrophotometric was used to determine MB by extrapolation of absorbance of MB calibration curve at wavelength of 662 nm. Different concentrations of MB (100-1000 ppm) were dissolved in 50 ml of PBS and stirred with 0.02 g of the titanium nanogels into a 100 ml conical flask at 25 °C. The filtrate samples were centrifuged and analyzed at different time intervals. The amount of dye adsorption at equilibrium Q (mg/g) and percent extraction (%E) was calculated from the following equation:

$$Q= [(C_o-C_e)xV/(m)] \quad (1)$$

$$\%E= [(C_o-C_e)x100/(C_o)] \quad (2)$$

Where C_o and Ce (mg/L) are the liquid phase concentrations of dye at initial and equilibrium, respectively, V (L) the volume of the solution and W (g) is the mass of adsorbent used.
The same procedure was repeated to determine the concentration of cobalt and nickel cations in aqueous solution using AAS.

2.5. Desorption studies

The TiO_2 nanogel composites after adsorption of first cycle were transferred into 0.05 N H2SO4 at 120 rpm for 1 h at 30◦C. The desorbed materials were washed with distilled water and the desorbed Ni (II), Co(II) and MB quantity was evaluated and the TiO_2 in the stripping medium was also detected using AAS. This procedure was repeated five cycles.

3. Results and discussion

Preparation of spherical titanium dioxide nanomaterials becomes big challenge to modify its surface for enhancing their surface properties to apply in the environmental technology. In the present work, the surface TiO_2 can be modified with nanogels to obtain reactive 3-D nanomaterials. We proposed the following Scheme 1 to form TiO_2 nanogel composites. It shows that the TiO_2 reacts with PVP or acrylamide monomers due to hydrogen bonding between the hydroxyl groups in TiO_2 and amide groups on the PVP and monomer surfaces. MBA and APS were used as crosslinker and initiator, respectively to encapsulate the TiO_2 into nanogel to obtain reactive nanocomposites. In case of polymerization of ionic monomer such AMPS-Na it was also expected that there is an interaction existed between the positively charged surface Ti-OH groups of TiO_2 and the negatively charged sulfonic acid groups [38].

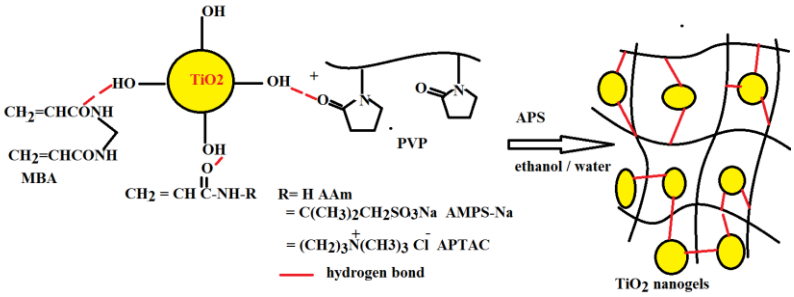

Scheme 1: Synthesis of TiO2 nanogel composites.

3.1. Characterization of titanium dioxide nanogel composites

It is very important to study the effect of crosslinking polymerization on the morphology of TiO_2 as represented by TEM photos (Fig. 1 a-e). The TiO_2 nanoparticles coated with PVP (Fig. 1 a) shows a clear interface among the particles which piles up the TiO_2 together loosely instead of aggregation obtained with TiO_2 without PVP. This result indicates that PVP cannot completely form disperse TiO2 nanoparticles as illustrated in (Scheme 1). The TEM photo of modified TiO_2 with PAAm (Fig. 1b), shows formation of TiO_2 nanocomposites has a spherical morphology with the formation of different sizes. This result indicates that PAAm assists to form partially dispersed nanocomposites. The modifications of TiO_2 with PAMPS-Na and PAMPS-Na/AAm produced different morphologies as illustrated in Fig. 1 c and d. The results suggest that AMPS-Na plays an important role to lead to well-dispersed TiO_2 nanocomposites with much smaller particle size than that obtained with PAAm. The nanocomposites nature of PAMPS-Na/TiO_2 (Fig. 1c) was illustrated from the high resolution lattice fringes with an interlayer distance of 0.15 nm, extremely close to the lattice spacing of the (1 0 1) plane in anatase TiO_2 [38]. Moreover, different morphologies as well defined spherical and stretched spherical obtained from modification of TiO_2 with PAMPS-Na/AAm. These results agree with the reported data for the preparation of highly dispersed and nanosized TiO_2 composites [39]. The morphology of PAPTAC-AAm/TiO_2 (Fig. 1e) was spherical and partially dispersed in water that can be referred to the repulsion between surface charges of TiO_2 and APTAC decreases the encapsulation of titanium into the nanogel composites, consequently, the TiO_2 tend to form agglomerates.

The surface morphology of the TiO_2 nanogel composites can be also determined from SEM photos as illustrated in Fig. 2a -c. The TiO2 showed needle morphology (Fig. 3a). The photos of TiO_2 nanocomposites based on PAMPS-Na/AAm and PAPTAC-AAm (Fig. 2b and c, respectively) were selected to show the effect of nanogel surface charges on the surface morphology of TiO_2particles. It was observed that the TiO_2 nanoparticles were firmly attached on the PAMPS-Na/AAm surfaces by self-assembly. While, the TiO_2 nanoparticles have heterogeneous distribution on PAPTAC-AAm surfaces (Fig. 2c) and the surface morphology had a scaly, thin, sheet-like appearance. Moreover, the surface showed non-uniformly distributed pores. These non-uniform pores can be referred to repulsive forces between surface positive charges of PAPTAC-AAm and TiO_2 which restricted bonding between the nanocomposite surfaces. This morphology was refereed to formation of agglomerated cluster-like structures due to the presence of high inorganic nanoparticle contents [40-41].

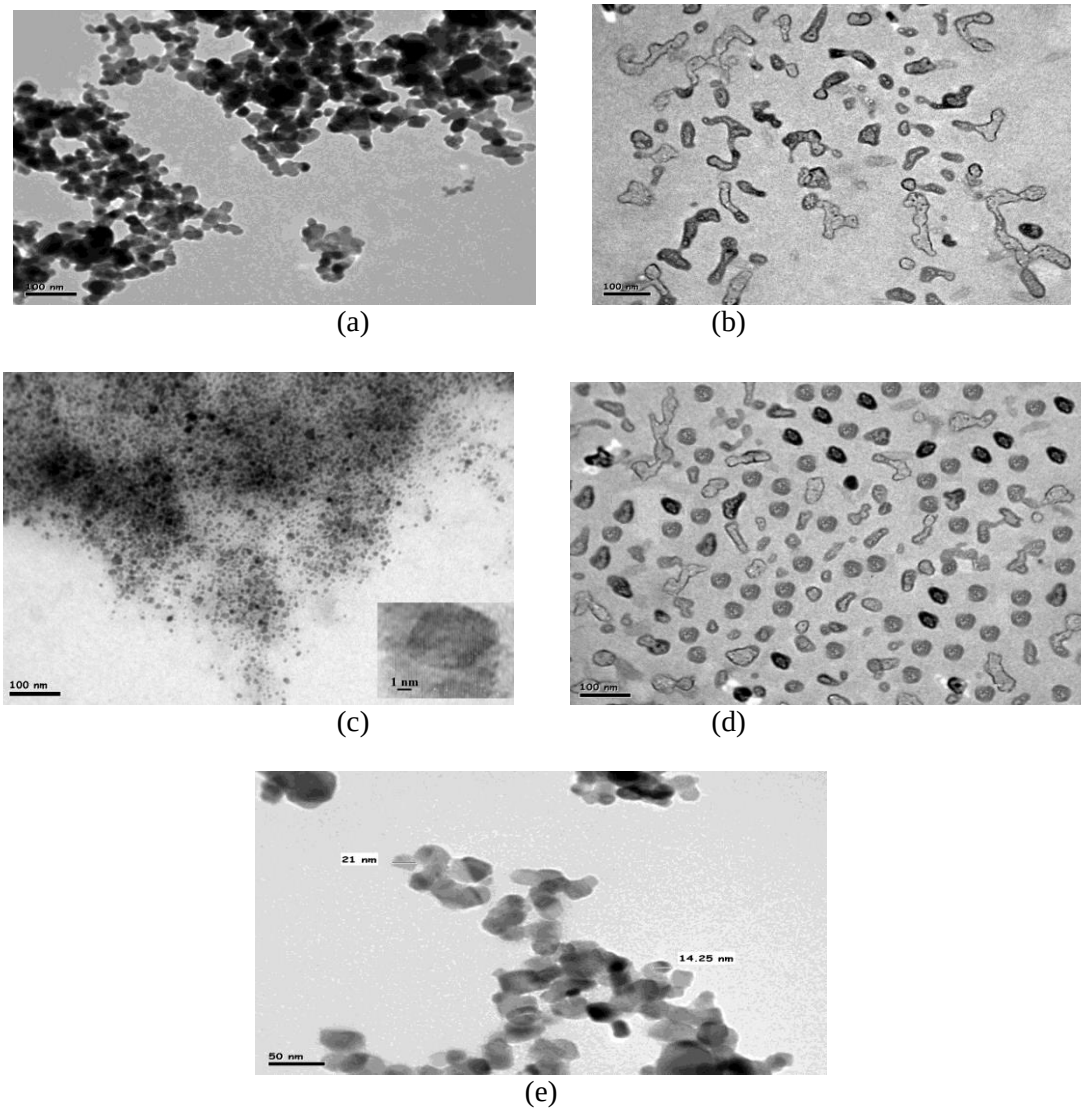

Fig.1. TEM micrographs of a) TiO_2, b) TiO_2 PAAm, c) TiO_2 PAMPS-Na (d) TiO_2 PAMPS-Na/AAm and e) TiO_2 PAPTAC/AAm.

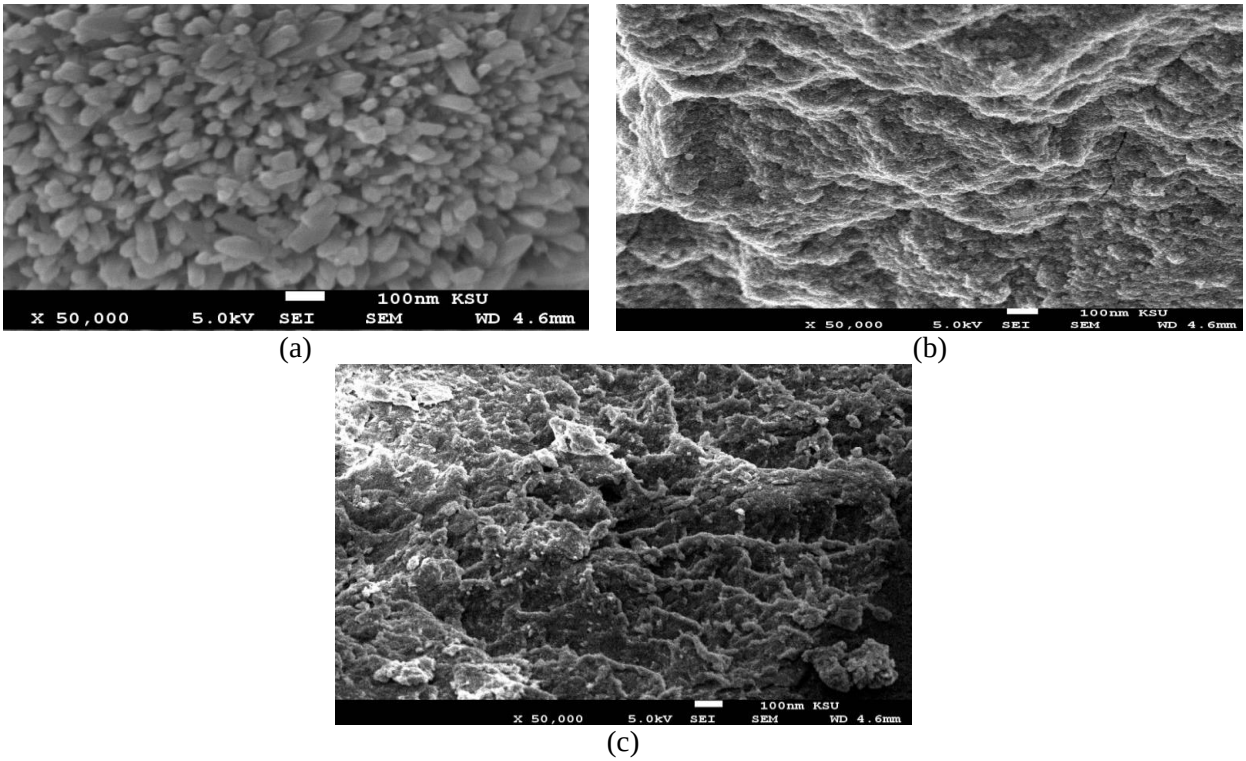

Fig.2. SEM photos of a) TiO_2, b) TiO_2 AMPS-Na/AAm and c) TiO APTAC/AAm nanogel composites.

The thermogravimetric analysis is a useful technique to determine the TiO_2 content and polymer degradation stability as confirmed from Fig. 3 and Table 1. The weight loss (Wt. %) of TiO_2 nanoparticles was around 4 % below 250◦C which was ascribed to the release of water that was physio-absorbed in the titanium [42]. The quantity of water was increased with nanogel composites to be 10 % which can be referred to the hydrophilicity of nanogels and their affinity to absorb water even humid water. The decomposition and water or ammonia losses from nanogel polymers started at temperature of 250 to 550 ◦C. During this stage, the weight loss between 220 and 290◦C was used to confirm the water lost that attributed to the decomposition of the amorphous hydrolytic compound when the anatase type TiO_2 crystals were formed. Moreover, the TiO_2 contents can be determined at temperature of 550◦C and the weight loss above this temperature can be referred to the endothermal phenomenon occurred from trans-formation of anatase TiO_2 into rutile TiO_2 [43]. The data listed in Table 1 indicated that the TiO_2 contents can be arranged in the order PAMPS-Na> PAAm > PAMPS-Na/AAm > PAPTAC/AAm nanogels. The TGA data also indicated that the weight losses of polymers of PAMPS-Na/AAm exhibited slow and partial loss of the organics up to 800◦C which indicates that TiO_2 have strong interaction with contents can be arranged in the order PAMPS-Na/AAm more than other nanogels.

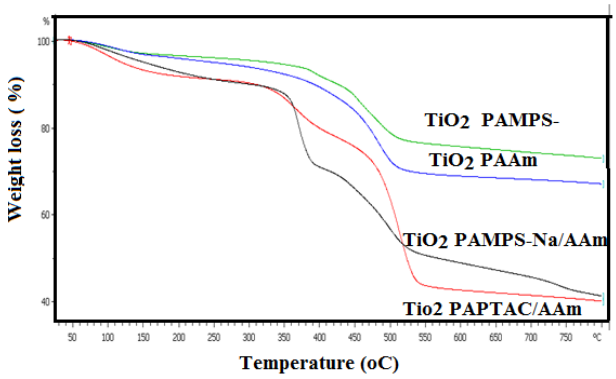

Fig.3. TGA thermograms of TiO_2 nanogel composites.

Table1. TGA data of amphiphilic titanium dioxide nanogel composites.

TiO_2 Nanogels modifier	Remaining		TiO_2 contents (Wt%)
	Temperature range ^oC	Weight loss (Wt%)	
PAMPS-Na	25-250	4	77
	250-550 ^oC	19	
	550-750 ^oC	3	
PAAm	50-250	6	69
	250-550	25	
	550-750	2	
PAMPS-Na/AAm	50-250	10	50
	250-550	40	
	550-750	7	
PAPTAC/AAm	50-250	10	42
	250-550	48	
	550-750	2	

3.2. Surface activity of Amphiphilic TiO_2 Nanogels

In our previous works [44-46] we succeeded to increase the surface activity of the inorganic nanoparticles by forming nanogel composites. Moreover, it was found that the nanogels achieved good results to reduce the surface tension of both water and nonpolar solvents such as hexane and toluene [47-49]. These amphiphilic nanogel composites showed high performance as emulsifiers, dispersants, corrosion inhibitors and water purification [44-49]. The surface activity of amphiphilic TiO_2 nanogel composites was determined after repeated purification to ensure that the encapsulated nanogels with TiO_2 are responsible for reduction of water surface tension. However, the relation between surface tension of water (γ; mN/m) and different amphiphilic concentration (-ln c; mol/L) was used to determine the ability of nanogel composites to disperse, aggregate or adsorb at interfaces. In this respect, this relation was plotted for TiO_2 nanogels and represented in Fig.4. Moreover, the critical aggregation concentration data (cac; mol/L) which represents the rapid change in γ value with dilution of nanogel composite concentration (as indicated in Fig.5) as

surface tension at cac (γ_{cac}; mN/m) and slope of curves ($-\partial \gamma / \partial \ln c$) were determined at 25 ^{o}C and listed in Table 2. The efficiencies of TiO2 nanogels to reduce the water surface tension was determined from the relation ($\Delta\gamma = \gamma_{o} - \gamma_{cac}$; mN/m where γ_{o} is the surface tension of water at 25 ^{o}C which equal 72.1 mN/m). Careful inspection of data confirmed that the TiO_2 PAMPS-Na/AAm nanogel composite has been greatly reduced the water surface tension at lower cac value. This can be attributed to the uniform distribution of nanogel particle size and strong interactions between TiO_2 and functional groups of PAMPS-Na/AAm as clarified from TEM and TGA data, respectively.

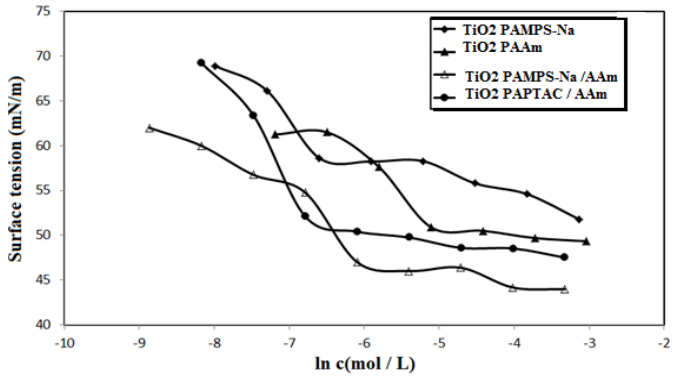

Fig.4. Adsorption isotherms of TiO_2 nanogel composites at 25 ^{o}C.

The ability of TiO_2 nanogels to adsorb at air water interface can be assigned from the values of concentration of the silica nanogel composites at the liquid–air interface (Γ_{max}) and the minimum area of silica nanogel composites (A_{min}). The Γ_{max} and A_{min} values were determined from equations 3 and 4[50],

$$\Gamma_{max} = (-\partial \gamma / \partial \ln c)_T / RT \quad (3)$$

$$A_{min} = 10^{16} / N \Gamma_{max} \quad (4)$$

where *R, T and N are* the temperature (K), the universal gas constant (in J mol^{-1} K^{-1}) and Avogadro's number, respectively. The Γ_{max}, A_{min}, and ($-\partial \gamma / \partial \ln c$) of TiO_2 nanogels were calculated and gathered in Table 2. The data of Γ_{max}, and A_{min}, confirmed that the TiO_2 nanogels based on PAMPS-Na and PAMPS-Na/AAm nanogels have greater tendency to adsorb at interface with lower A_{min} values than other type of TiO_2 nanogels. This can be attributed to the ability of sulfonate groups PAMPS-Na facilitates the adsorption of TiO_2 nanogels at interface due to strong interaction between TiO_2 nanoparticles and nanogels. Finally, it can be concluded that the strong interactions between TiO_2 nanoparticles and nanogels will increase the amphiphilic character of nanogel composites.

Table 2. Surface activity parameters of titanium dioxide nanogels in water at 25 ^{o}C

.

Titania Nanogels modifier	cac mol/L x 10^3	γ_{cac} mN/m	$\Delta\gamma = \gamma_{o} - \gamma_{cac}$ mN/m	($-\partial \gamma / \partial \ln c$)	Γ_{max} x 10^{10} mol/ cm^2	A_{min} nm^2/ molecule
P-AMPSNa	5.4	55.1	17.0	5.2	2.1	0.790
PAAm	6.02	50	22.1	3.43	1.4	1.190
PAMPS-Na/AAm	2.3	45.5	26.6	8.59	3.5	0.473
PAPTAC/AAm	4.5	48.6	23.5	4.08	1.9	0.880

3.3 Application of amphiphilic TiO_2 nanogels water treatment

Titanium dioxide and its composites attracted great attention to control water pollutant, especially organic dyes, by photo degradation from dye containing solutions [51-53]. The main drawback of the photo degradation of organic dyes concerned with the production of hazardous reactive intermediates after decolourization of dyes which could not be removed by photo catalysis or using pro-longed UV irradiation only. Moreover, the application of adsorbents or conventional methods (such as coagulation, filtration, biological treatment, chlorination, ozonation and flocculation) are not sufficient for water treatment due they are not being cost-effective and only transfer the pollutants from water phase to another with applying further treatment. To overcome these drawbacks of both photo degradation and adsorbents, the present work synthesized amphiphilic TiO_2 nanogels have strong ability to uptake organic and inorganic pollutants and used as photocatalyst to remove the dye residual that was not removed from water. This also assists the adsorbents to remove the intermediates formed from dye degradations.

It is necessary to optimize the adsorption conditions that assist to increase the performance of adsorbents. In this respect, pH of solutions plays an important rule to optimize the removal of either organic or inorganic pollutants from water by static charge or complexation mechanisms, respectively. The surface charges of nanogel composites play an important rule for removal of charged cation dyes such as MB. In this respect, Zeta potential (mV) of TiO_2 with and without nanogels was measured at different pH solution at constant temperature, ionic strength and 0.001 M of KCl and represented in Fig.5. The relation between zeta potential and pH (Fig. 6) can be used to determine the pH at which the TiO2 nanoparticles possessed zero charge which knows as the point of zero charge (PZC). The pH at PZC for TiO2 nanoparticles were determined and listed in Table 3 which indicates that TiO2 PAMPS-Na nanocomposite has lowest PZC**.** The low PZC value confirms the increment of hydroxyl group concentrations on the surface of bind TiO2 with nanogel composites [54]. The data confirmed that the pH 8-9 was optimum to cover the TiO_2 with sufficient negative charges able to remove cationic organic and inorganic pollutants and to highly disperse the adsorbents into the solutions to increase their performance. It was previously reported that the optimum zeta potential to produce dispersed nanoparticle was more than + 30 or less than -30 mV [44]. The data in Fig. 6 confirm that all TiO_2 nanocomposites possess positive charges in acidic medium and negative charges in basic medium above pH 8. This could be referred to the presence of Ti ions in tetrahedral coordination, which can act as Lewis acid sites. Moreover, the deionization of sulfonate and protonation of amide groups of nanogels could be occurred in acidic medium. It was also observed that both TiO_2 modified with PAMPS-Na and PAMPS-NA/AAm have high stable zeta potential to obtain highly dispersed nanogel composites and the optimum pH for applying the prepared nanocomposite is 9.

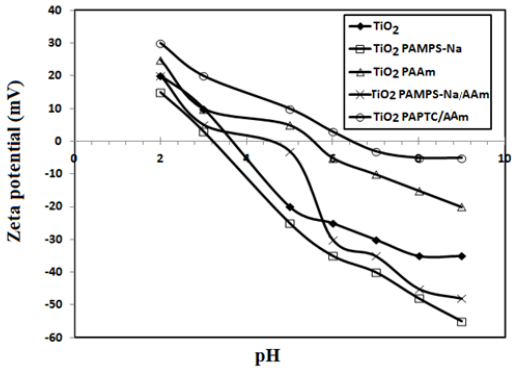

Fig.5. Relation between zeta potential of TiO_2 nanogel composites at 25 ^oC in 0.001 M KCl.

Table 3: Removal data of 1000 ppm MB, Co (II) and Ni (II) from water at pH 9 and temperature of 25 ^oC.

	PZC	MB		Co (II)		Ni (II)	
		Q max	Time	Q max	Time (minute)	Q max	Time (minute)
TiO_2	3.8	11	60	9	60	5	60
TiO_2 PAMPS-Na	3.2	399	70	350	60	282	90
TiO_2 PAAm	5.6	372	240	340	300	330	260
TiO_2 PAMPS-Na/AAm	4.4	445	40	488	50	455	30
TiO_2 APTAC/AAm	6.4	423	90	345	120	390	100

The effect of pH on sorption capacities q max (mg/g) of the prepared TiO_2 and nanogel composites for MB and inorganic cations (Co^{2+} and Ni^{2+}) at different pH was evaluated and listed in Table 3. It was found that the sorption capacity of MB increased with increasing pH of solution from 3 to 9. This result indicates that the MB was removed from water by attraction mechanism between negative charges of TiO_2 surfaces and positive charges of cationic dyes. It was also suggested that there is a hydrogen bond formed between polar groups of MB and amide or sulfonate groups of nanogels. While the removal of both Co and Ni cations could be removed through surface complexation mechanism as indicated from the strong adsorption of MB, Ni and Co cations at pH > PZC. The formation of complex between heavy metal cations and TiO_2 nanogel composites can be illustrated in Scheme 2. It was proposed that the adsorption of heavy metal was carried out primarily due to the interaction between - NH group of nanogels and Co^{2+} or Ni^{2+} and Ti- O on the nanocomposite.

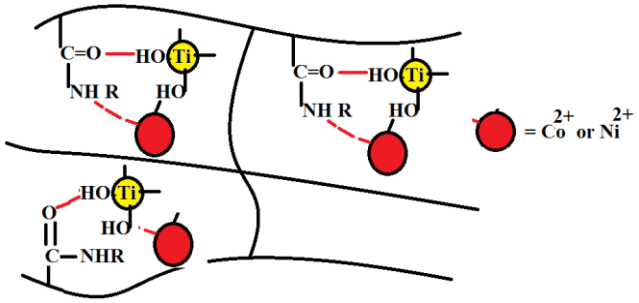

Scheme 2. Interaction between TiO2 nanogel composites and Ti (II) or Ni (II) cations.

3.4. Adsorption Desorption isotherms

Careful inspection of data listed in Table 3 proved that the TiO_2 PAMPS-Na/AAm nanogel composite has great affinity to adsorb both MB and heavy metal cations more than other nanogel composites although it contains 50 (Wt. %) of TiO2 contents as indicated from TGA data (Table 2). It was expected that the low TiO_2 contents in nanogel composites increases the interactions between polar groups of nanogels and MB or heavy metal. Therefore, the sorption capacity assets of nanogel composites decreased with increasing titanium NP content. Consequently, the nature of adsorption process of adsorbate on the surface of adsorbent is very important parameter to control the pollutant removal from aqueous solution. There are two common models of Langmuir and Freundlich are the most widely used models to describe the adsorption of adsorbate on the adsorbents surfaces. The Langmuir and Freundlich isotherms are given by Eq. (5) and (6), respectively [55-56]

$$(C_e/Q_e) = [(1/Q_{max}\, K_l) + (C_e/Q_{max})] \quad (5)$$

$$\log (Q_e) = \log (K_f) + [(1/n) \times \log (C_e)] \quad (6)$$

where Q_e, Q_0, C_e, n, K_l and K_f are the equilibrium and maximum amount of dye (mg/g) adsorbed on TiO_2 nanogel composites, the concentration of dye solution at equilibrium (mg/L), empirical constant , Langmuir and Freundlich constants, respectively. The adsorption intensity of adsorbate on the adsorbent surfaces was estimated from 1/n values. The relations of Ce/Qe against Ce and ln *Qe* versus ln *Ce* are gathered and illustrated in Fig. 6. The Langmuir and Freundlich constants are determined and listed with the experimental Q_{max} and % E in Table 4. The R^2 data (Table 4) indicated that the sorption of MB homopolymer based on PAAm and PAMPS-Na is more fitted to Langmuir isotherm rather than Freundlich isotherm. While the copolymerization of AAm with AMPS-Na or APTAC monomer fitted Freundlich isotherm more than Langmuir isotherm. This means that the reactivity ratios between different monomers produced heterogeneous nanogel composite surfaces and form multilayer of adsorbate on the adsorbent surfaces. The nanogels based on homopolymers of PAAm or PAMPS-Na produce homogeneous surfaces and the adsorbate based on MB or heavy metal from monolayer to cover the TiO_2 nanogel composites [57].

It is of interest to study the economic feasibility or reusability of nanocomposite to reprocess for pollutants removal up to n number of cycles without activation or destruction the mechanical or chemical characteristics. In this respect, a desorption of MB or heavy metal from TiO_2 nanogel composites was detached during 30 minute in the first cycle by treating with 0.05 N H_2SO_4 that competing with the MB or Ni and Co ions for the binding sites. The nanogel composite based on TiO_2 PAMPS-Na/AAm was selected as better adsorbent to investigate its reusability for different cycles. The desorption study confirmed that the TiO_2 nanoparticles were not leached from the nanogel composites. The desorption study confirmed that the TiO_2 PAMPS-Na/AAm lost approximately 3, 5 and 8 % from its initial efficiency after 5 cycles for MB, Ni and Co ions, respectively. Therefore, we can conclude that the physically adsorbed MB was desorbed while the electrostatic and complexation reactions occurring between the TiO_2 nanocomposites and the MB or Ni (II) and Co (II) prevented complete desorption.

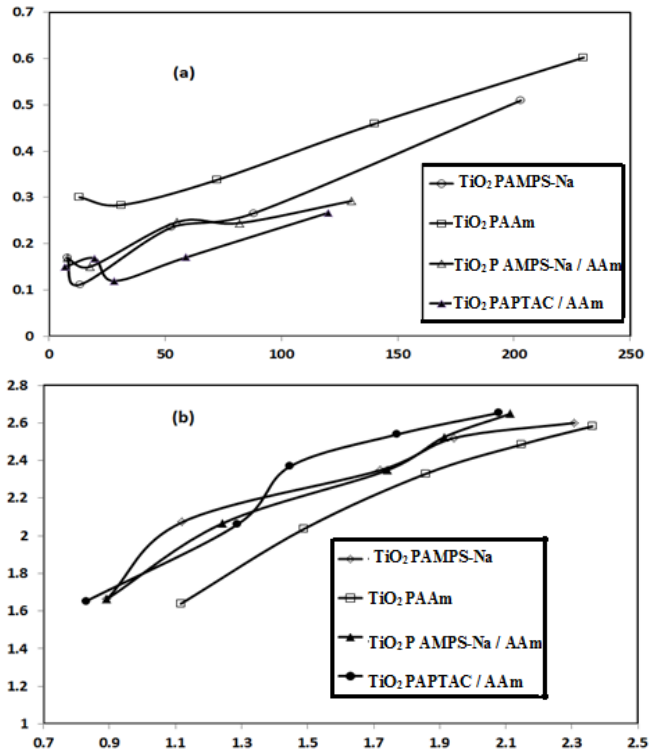

Fig. 6. Adsorption isotherms of TiO_2 nanogel composites a) Langmuir and b) Freundlich models used for removal MB from aqueous solution at 25 ^oC.

Table 4. Adsorption isotherm parameters for removal of 1000 ppm of MB dye using titanium nanogels at 25 ^oC.

Adsorbents	Langmuir isotherm parameters			Freundlich isotherm parameters		
	Q_{max} mg/g	K_l L/mg	R^2	1/n	K_f	R^2
TiO_2 PAMPS-Na	526	0.0157	0.9878	0.624	0.093	0.918
TiO_2 PAAm	666	0.0059	0.998	0.753	0.064	0.942
TiO_2 P AMPS-Na / AAm	909	0.0076	0.885	0.778	0.008	0.983
TiO_2 PAPTAC / AAm	833.3	0.0093	0.895	0.833	0.0046	0.960

4. Conclusions

The present work prepared new titanium dioxide nanogel composites have strong tendency to adsorb the water pollutants beside their application as photocatalyst to remove water pollutants. TiO_2 was encapsulated into nanogel to form spherical and high dispersed nanocomposites. The repulsion between surface charges of TiO_2 and APTAC decreases the encapsulation of titanium into the nanogel composites. The TiO_2 contents were arranged in the order PAMPS-Na> PAAm > PAMPS-Na/AAm > PAPTAC/AAm nanogels. The TGA data also indicated that the TiO_2 have strong interaction with PAMPS-Na/AAm contents more than other nanogels. The surface activity data confirmed that the TiO_2 nanogels based on PAMPS-Na and PAMPS-Na/AAm nanogels have greater tendency to adsorb at interface with lower A_{min} values than other type of TiO_2 nanogels. This was referred to the ability of sulfonate groups PAMPS-Na facilitates the adsorption of TiO_2 nanogels at interface due to strong interaction between TiO_2 nanoparticles and nanogels. Finally, it can be concluded that the strong interactions between TiO_2 nanoparticles and nanogels will increase the amphiphilic character of nanogel composites. The TiO_2 nanogels based on homopolymers of PAAm or PAMPS-Na produce homogeneous surfaces and the adsorbate based on MB or heavy metal from monolayer to cover the TiO_2 nanogel composites.

Acknowledgment

The project was financially supported by King Saud University, Vice Deanship of Research Chairs.

References

[1] S. Yang, X. Yang, X. Shao, R. Niu, L. Wang, , J. Hazard. Mater.**186**, 659 (2011).
[2] S. Chatterjee, S. Lim, S.H. Woo, Chem. Eng. J. **160**, 27 (2010).
[3] F. Han, V.S.R. Kambala, M. Srinivasan, D. Rajarathnam, R. Naidu, Appl. Catal. A: Gen. **359**, 25 (2009).
[4] S. Yang, P. Wang, X. Yang, L. Shan, W. Zhang, X. Shao, R. Niu, , J.Hazard. Mater. **179**, 552 (2010).
[5] S. Zhan, D. Chen, X. Jiao, C. Tao, J. Phys.Chem. B **110**, 11199 (2006).
[7] J.S. Hu, L.L. Ren, Y.G. Guo, H.P. Liang, A.M. Cao, L.J. Wan, Ch.L. Bai, Chem. Int. Ed. **44**, 1269 (2005).
[8] A. Khan, L. Sajjad, S. Shamaila, J. L. Zhang, J. Hazard. Mater. **235–236**, 307 (2012).
[9] P. Zhang, C.L. Shao, X.H. Li, M.Y. Zhang, X. Zhang, Y.Y. Sun, Y.C. Liu, J. Hazard. Mater. **237–238**, 331 (2012).
[10] B.-H. Jeong, E. Hoek, Y. Yan, A. Subramani, X. Huang, G. Hurwitz, A.K. Ghosh, A. Jawor, J. Membr. Sci. **294**, 1 (2007).
[11] A.K. Ghosh, B.-H. Jeong, X. Huang, E. Hoek, J. Membr. Sci. **31**,134 (2008).
[12] D. Emadzadeh, W.J. Laua, M. Rahbari-Sisakht, A. Daneshfar, M. Ghanbari, A. Mayahi, T. Matsuura, A.F. Ismail, Desalination **368**,106 (2015).
[13] N. Ma, J. Wei, R. Liao, C.Y. Tang, J. Membr. Sci. **405–406**, 149 (2012).

[14] H.S. Lee, S.J. Im, J.H. Kim, H.J. Kim, J.P. Kim, B.R. Min, Desalination **219**,48 (2008).
[15] G. L. Jadav, P.S. Singh, J. Membr. Sci. **328**, 257 (2009).
[16] M. Ben-Sasson, X. Lu, E. Bar-Zeev, K.R. Zodrow, S. Nejati, G. Qi, E.P. Giannelis, M. Elimelech, Water Res. **62**, 260 (2014).
[17] D. Emadzadeh, W. Lau, A. Ismail, Desalination **330**, 90 (2013).
[18] E. Dujardin, S. Mann, Bio-inspired materials chemistry, Adv. Mater. **14**, 775 (2002).
[19] J. S. Hu, Y.G. Guo, H.P. Liang, L. J. Wan, L. Jiang, J. Am. Chem. Soc. **127**, 17090 (2005).
[20] B.V. Adersson, A. Herland, S. Masich, O. Ingans, Nano Lett. **9**, 853 (2009).
[21] T. Kasuga, M. Hiramatsu, A. Hoson, T. Sekino, K. Niihara, Langmuir **14**, 3160 (1999).
[22] J. Wang, Z.Q. Lin, Chem. Mater. **20**, 1257 (2008).
[23] W.T. Sun, Y. Yu, H.Y. Pan, X.F. Gao, Q. Chen, L.M. Peng, J. Am. Chem. Soc. **130**, 1124 (2008).
[24] X.J. Feng, K. Shankar, O.K. Varghese, M. Paulose, T.J. Latempa, C.A. Grimes, Nano Lett. **8**, 3781 (2008).
[25] J. Li, H.C. Zeng, J. Am. Chem. Soc. **129**, 15839 (2007).
[26] H. Ming, Z. Ma, H. Huang, S.Y. Lian, H.T. Li, X.D. He, H. Yu, K.M. Pan, Y. Liu, Z.H. Kang, Chem. Commun. **47**, 8025 (2011).
[27] B. Smarsly, D. Grosso, T. Brezesinski, N. Pinna, C. Boissière, M. Antonietti, C. Sanchez, Chem. Mater. **16**, 2948 (2004).
[28] Y.J. Cheng, L.J. Zhi, W. Steffen, J.S. Gutmann, Chem. Mater. **20**, 6580 (2008).
[29] Z. K. Zheng, B. B. Huang, X.Y. Qin, X.Y. Zhang, Y. Dai, Chem.Eur. J. **16**, 11266 (2010).
[30] Y.W. Wang, L.Z. Zhang, K.J. Deng, X.Y. Chen, Z.G. Zou, J.Phys. Chem. C **111**, 2709 (2007).
[31] G.H. Tian, Y.J. Chen, W. Zhou, K. Pan, C.J. Tian, X.R. Huang, H.G. Fu, Cryst. Eng. Commun. **13**, 2994 (2011).
[32] L.S. Zhong, J.S. H, L.J. Wan, W.G. Song, Chem. Commun.**13**, 1184 (2008).
[33] A. M. Atta, O. E. El-Azabawy and H.S. Ismail, Corrosion science, **53**, 1680 (2011).
[34] A. M. Atta, R. A. M. El-Ghazawy, R. K. Farag and Sh. M..Elsaeed, polymer advanced technologies, **22**, 732 (2011).
[35] A. M. Atta, Journal of Applied Polymer Science, **124**, 3276 (2012).
[36] M. A. Akl, A.A. Sarhan, K. R. Shoueir, A. M. Atta, J Disp Sci Technologies **34**, 1399 (2013)**.**
[37] M. A Akl, A. M Atta, A. F. M Yousef and M. I. Alaa, Polym Int **62**, 1667 (2013).
[38] X. Yang, F. Ma, K. Li, Y. Guo, J. Hu, W. Li, M. Huo, Y. Guo, Journal of Hazardous Materials **175**, 429 (2010).
[39] X. Yang, Y. Wang, L. Xu, X. Yu, Y. Guo, J. Phys. Chem. C **112**, 11481 (2008).
[40] S. Kango, S. Kalia, A. Celli, J. Njuguna,Y. Habibi,R. Kumar, Prog. Polym.Sci. **38**, 1232 (2013).
[41] H. J. Kim, K. Choi, Y. Baek, D. G. Kim, J. Shim, J. Yoon, ACSAppl. Mater. Interfaces **6**, 2819 (2014).
[42] X. Wang, Q. Ye, T. Gao, J. Liu, F. Zhou, , Langmuir **28**, 2574 (2012).
[31] A.E. Langroudi, A. Rabiee, A novel acrylamide-anatase hybrid nanocomposite,J. Polym. Res. **19**, 9970 (2012).
[43] X. Wang, D. Hu, J. Yang, Chem. Mater. **19**, 2610 (2007).
[44] A. M. Atta, H. A. Al-Lohedan, Z.A. ALOthman, A. A. Abdel-Khalek, A. M. Tawfeek, Journal of Industrial and Engineering Chemistry, **31**, 374 (2015).
[45]A. M. Atta, G. A. El-Mahdy. and H. A. Al-Lohedan, Int. J. Electrochem. Sci., **10**, 102 (2015).
[46] G. A. El-Mahdy, A. M. Atta, , H. A. Al-Lohedan, A. M. Tawfik, A. A. Abdel–khalek, Int. J. Electrochem. Sci., **10**, 151 (2015).
[47] A. M. Atta, A. K. F. Dyaba, and H. A. Allohedan, Polymer for Advanced technol**.** **24**, 986 (2013)**.**
[48] A. M. Atta, M. A. Akl, A. M. Youssef, M. A. Ibraheim, Adsorption Science & Technology, **31**, 397-419 (2013).
[49] A. M. Atta, A. K. F. Dyab, H. A. Al-Lohedan, Polymer Science, Ser. B, **56**, 770 (2014).
[50] M. J. Rosen. Surfactants and Interfacial Phenomena, John Wiley, New York,

(1985) 15-55.
[51] A.K. Gupta, A. Pal, C. Sahoo, Dyes Pigments **69**, 224 (2006).
[52] T.S. Natarajan, M. Thomas, K. Natarajan, H.C. Bajaj, R.J. Tayade, Chem. Eng. J. **169**, 126 (2011).
[53] I.K. Konstantinou, T.A. Albanis, Appl. Catal. B: Environ. **49**, 1 (2004).
[54] J.C. Yu, L.Z. Zhang, Z. Zheng, J.C. Zhao, Chem. Mater. **15**, 2280 (2003).
[55] I. Langmuir. J. Am. Chem. Soc. **40**, 1361 (1918).
[56] H. M. F. Freundlich. Z Phys Chem. **57**, 385 (1906).
[57] C.H. Giles, A.P. D'Silva, I. Easton.. J. Coll. Interface Sci. **47**, 766 (1974).